DISCRETE AND CONTINUOUS
DYNAMICAL SYSTEMS
Volume **39**, Number **7**, July **2019**

doi:10.3934/dcds.2019172

pp. **X–XX**

# A POLYGONAL SCHEME AND THE LOWER BOUND ON DENSITY FOR THE ISENTROPIC GAS DYNAMICS

Geng Chen

Department of Mathematics, University of Kansas
Lawrence, KS 66045, USA

Ronghua Pan*

School of Mathematics, Georgia Institute of Technology
Atlanta, GA 30332, USA

Shengguo Zhu

Mathematical Institute, University of Oxford
Oxford, OX2 6GG, UK

(Communicated by the associate editor name)

Abstract. Positive density lower bound is one of the major obstacles toward large data theory for one dimensional isentropic compressible Euler equations, also known as p-system in Lagrangian coordinates. The explicit example first studied by Riemann shows that the lower bound of density can decay to zero as time goes to infinity of the order $O(\frac{1}{1+t})$, even when initial density is uniformly positive. In this paper, we establish a proof of the lower bound on density in its optimal order $O(\frac{1}{1+t})$ using a method of polygonal scheme.

1. **Introduction.** In this paper we consider the Cauchy problem for isentropic gas dynamics in Lagrangian coordinates

$$\begin{cases} v_t - u_x = 0 \\ u_t + p(v)_x = 0\,, \\ v(x,0) = v_0(x), \quad u(x,0) = u_0(x)\,, \end{cases} \tag{1}$$

where the specific volume $v = 1/\rho$, the density $\rho > 0$ and the velocity $u$ of the gas are all functions of $(x,t) \in \mathbb{R} \times \mathbb{R}^+$. The pressure $p(v)$ satisfies

$$p(v) = Kv^{-\gamma} \quad \text{with} \quad \gamma > 1\,, \tag{2}$$

where $\gamma$ is the adiabatic constant, and $K$ is a positive constant. This system is also called the p-system. For Lipschitz continuous solutions, (1) is equivalent to the

2010 *Mathematics Subject Classification.* Primary: 76N15, 35L65; Secondary: 35L67.

*Key words and phrases.* Gas dynamics, p-system, singularity formation, vacuum, large data.

G. Chen is partially supported by National Science Foundation under grant DMS-1715012. R. Pan is partially supported by National Science Foundation under grants DMS-1516415 and DMS-1813603, and by National Natural Science Foundation of China under grant 11628103. S. Zhu is partially supported by National Natural Science Foundation of China under grants 11231006 and 11571232, Natural Science Foundation of Shanghai under grant 14ZR1423100, Australian Research Council grant DP170100630, Newton International Fellowships NF170015 and China Scholarship Council.

* Corresponding author.

corresponding Cauchy problem of isentropic Euler equations in Eulerian coordinates [23]. Letting

$$c = \sqrt{-p'(v)}$$

be the sound speed, the Riemann invariants $s$ and $r$ are defined as

$$s := u - \phi, \qquad r := u + \phi \tag{3}$$

with

$$\phi \equiv \phi(v) := \int_1^v \sqrt{-p'(v)}\, dv\,. \tag{4}$$

For smooth solutions, $s$ and $r$ satisfy

$$s_t + cs_x = 0 \quad \text{and} \qquad r_t - cr_x = 0\,.$$

Toward a large data theory, such as the existences of BV solutions for isentropic Euler equations (1), one of the main challenges comes from the possible degeneracy when density approaches zero. In fact, when solution approaches vacuum, system (1) loses its uniformly strict hyperbolicity, which causes major difficulties in analyzing the large data solutions, see [2,5,18] for analysis and examples showing these difficulties. Therefore, sharp information on the time decay of density lower bound is critical in the study of compressible Euler equations.

It is well known for (1) that the density can be arbitrarily close to zero as time goes to infinity, even when initial density is uniformly away from zero, such as in the interaction of two strong rarefaction waves, c.f. [9,20]. In his pioneer paper [20] of 1860, Riemann studied the interaction between two rarefaction waves. Based on Riemann's construction, when $\gamma = \frac{2N+1}{2N-1}$ with any positive integer $N$, Lipschitz continuous examples were provided in Section 82 of [9], in which density functions are proved to decay to zero in an order of $O(1+t)^{-1}$. For reader's convenience, a relative detailed discussion can be found in Section 2 below. Similar example can be found in [14] for any $\gamma > 1$. In this paper, for $1 < \gamma < 3$, we will prove the sharp positive density lower bound of the order $O(1+t)^{-1}$ for any Lipschitz continuous solutions of (1).

Thanks to the elegant structure of Euler equations, the local behavior of smooth solutions can be classified into two classes: compression and rarefaction, as defined below, see for instance [4,8,15,21]. These concepts can be generalized to Lipschitz continuous solutions without any difficulty.

**Definition 1.1.** At any point on $(x,t)$-plane, the smooth solution is forward (resp. backward) rarefaction $\overrightarrow{R}$ $(\overleftarrow{R})$ if and only if $s_x \geq 0$ (resp. $r_x \geq 0$) at that point; forward (resp. backward) compressive $\overrightarrow{C}$ $(\overleftarrow{C})$ if and only if $s_x < 0$ (resp. $r_x < 0$) at that point.

Among many results, two of them are closely related to this paper. For purely rarefactive piecewise Lipschitz continuous solutions, Lin [17] proved that the density has a $O(1+t)^{-1}$ order lower bound. For general smooth solutions, including compressions in the solution, in a very recent paper [7], we find a $O(1+t)^{-\frac{4}{(3-\gamma)}}$ lower bound when $1 < \gamma < 3$. This result helps us to prove that gradient blowup of $u$ and/or $v$ happens in finite time if and only if the initial data are forward or backward compressive somewhere. This latter result is further extended in [7] to nonisentropic flow.

In this paper, for general Lipschitz continuous solutions of (1) when $1 < \gamma < 3$, we improve the lower bound on density from $O((1+t)^{-\frac{4}{(3-\gamma)}})$ in [7] to the optimal

order of $O(1+t)^{-1}$. Based on this result, the estimate in [7] on the life-span for classical solutions of (1) can be improved.

Our main result of this paper is the following Theorem.

**Theorem 1.2.** *Let $1 < \gamma < 3$. Assume that initial data $s_0(x) = s(x,0)$ and $r_0(x) = r(x,0)$ are uniformly bounded and Lipschitz continuous functions on $x \in \mathbb{R}$, and denote that*

$$\max_{x\neq y} \frac{s_0(x) - s_0(y)}{x-y} = L_1 < \infty, \qquad \max_{x\neq y} \frac{r_0(x) - r_0(y)}{x-y} = L_2 < \infty$$

*and*

$$\max_x \big\{ |s_0(x)|, |r_0(x)| \big\} = L_3 < \infty.$$

*Furthermore, assume that $v(x,0)$ in the initial data has uniformly positive upper bound:*

$$\max_x v(x,0) = L_4 < \infty.$$

*For any given positive time $T$, if $\big(u(x,t), v(x,t)\big)$ is a Lipschitz continuous weak solution on $\mathbb{R}\times[0,T]$ for the initial value problem of (1), then there exists a positive constant $L = L(L_1, L_2, L_3, L_4)$, independent of $T$, such that*

$$v(x,t) \le \max_x \big(v(x,0)\big) + L\,t, \quad \text{for any} \quad (x,t) \in \mathbb{R}\times[0,T]. \tag{5}$$

Here, $L_1$ and $L_2$ measure how rarefactive the initial data are.

To prove this theorem, we study a polygonal scheme similar to those used in [17, 19]. The polygonal scheme was first introduced by Dafermos [11] in the study of scalar conservation law, then was modified by Diperna for system of conservation laws [12]. This scheme, under a renowned name front tracking, has been widely used for the well-posedness and behaviors of solutions for hyperbolic conservation laws. For more details on the development of front tracking method, see for instance [1, 10, 13, 22], and references therein.

The main difference of our scheme from the previous ones, is that we add a memory of the local rarefaction and compression character on our scheme, which helps us finally track the maximum rarefaction on waves. And this quantity is crucial in estimating the decay of density. Here, we choose the polygonal scheme since it fits the p-system very well. We wish to point out here that one of our motivations in this paper besides showing the density lower bound is to provide the readers a new method in tracking the variation of solutions during the wave interactions.

In order to track the density changes along the time evolution, it is important to characterize the key players of density loss in the approximate solutions. In the polygonal scheme, we divide the $(x,t)$-plane into finite districts, on each of which the forward (resp. backward) waves are of the same type: forward (resp. backward) rarefaction or compression.

Because the density increases when it crosses a compressive wave, it seems that only districts including forward and backward rarefaction waves directly make the density decreasing. However, things are more complicated than they appear. In fact, for rarefaction-rarefaction districts adjacent to initial line, we can apply directly a similar argument used in [17] to obtain the desired lower bound on density. However, the major difficulty that we have to conquer in this paper is how to analyze those rarefaction-rarefaction districts far away from the initial line. These rarefaction

waves have passed some compressions in the opposite families before reaching the rarefaction-rarefaction districts. So

$$\max_{x\neq y}\frac{s(x,t)-s(y,t)}{x-y} \quad \text{and} \quad \max_{x\neq y}\frac{r(x,t)-r(y,t)}{x-y},$$

might increase as time evolves. In order to obtain a sharp lower bound on density, we need to carefully analyze all three types of districts: rarefaction-rarefaction, rarefaction-compression and compression-compression districts.

Unlike many previous analysis, where the changes of density are monitored across the boundaries of districts, or jump edges, we track the wave packs in each district, for which we introduced the concepts of rarefactive and/or compressive characters in Section 3 below. With the help of these characters, we are able to track the variation of density precisely. Furthermore, in Definition 4.1, we introduced an interesting function $a(t)$ which measures the possible density loss. Using one of our key new ideas, we are able to prove in Lemma 4.3 that $a(t)$ is not increasing in time, in the scheme approximating general smooth solutions. Using this lemma, we could sew up the density estimates obtained in each district into a global one up to time $T$ in the regime of Lipschitz continuous solutions.

This paper is organized as follows. In Section 2, we review the explicit example given in [9] where density decays to zero in time with an order of $O(1+t)^{-1}$. In Section 3, we review the polygonal scheme and define Rarefaction/Compression character. In Section 4, we prove the main theorem on lower bound of density. Finally, as an application, in Section 5, we use the time-dependent lower bound (5) obtained in Theorem 1.2 to improve the life-span estimates for classical soluitons of (1) given in [7].

2. **Exact interaction between two centered rarefactions.** In this section, we review a classical example for interaction between two centered rarefaction waves provided in Section 82 of [9], where detail calculations are given. To be consistent with classical literatures, (only) throughtout this section, instead of $s$ and $r$, we use the following slightly different Riemann invariants $\mathcal{S}$ and $\mathcal{R}$,

$$\mathcal{S}=u+\tfrac{2\sqrt{K\gamma}}{\gamma-1}v^{\frac{1-\gamma}{2}}, \quad \mathcal{R}=u-\tfrac{2\sqrt{K\gamma}}{\gamma-1}v^{\frac{1-\gamma}{2}}. \tag{6}$$

In fact, $\mathcal{S}$ (resp. $\mathcal{R}$) is different from $s$ (resp. $r$) only by some constants. The following relation is crucial to measure density,

$$\mathcal{S}-\mathcal{R}=\tfrac{4\sqrt{K\gamma}}{\gamma-1}v^{\frac{1-\gamma}{2}}. \tag{7}$$

For simplicity, in Figure 1 below, we only consider an interaction between two centered rarefaction waves, where we assume that the first interaction happens at $t=\bar{t}>0$ and $x=0$, with constant state $(\bar{\mathcal{S}},\bar{\mathcal{R}})$ below the point $(0,\bar{t})$. Furthermore, we assume that $u(0,\bar{t})=0$, hence

$$\bar{\mathcal{S}}=-\bar{\mathcal{R}}>0.$$

Again, for simplicity, we assume that $\mathcal{S}$ in the left state of interaction is always positive and $\mathcal{R}$ in the right state of interaction is always negative.

Then using the fact that $\mathcal{S}$ and $\mathcal{R}$ are constant along forward and backward characteristics, respectively, in [20], Riemann first found the following equation:

$$t(\mathcal{S},\mathcal{R})=\bar{t}\left(\frac{\bar{\mathcal{S}}-\bar{\mathcal{R}}}{\mathcal{S}-\mathcal{R}}\right)^{\sigma}F\left(1-\sigma,\sigma,1,\frac{(\bar{\mathcal{S}}-\mathcal{S})(\bar{\mathcal{R}}-\mathcal{R})}{(\bar{\mathcal{S}}-\bar{\mathcal{R}})(\mathcal{S}-\mathcal{R})}\right) \tag{8}$$

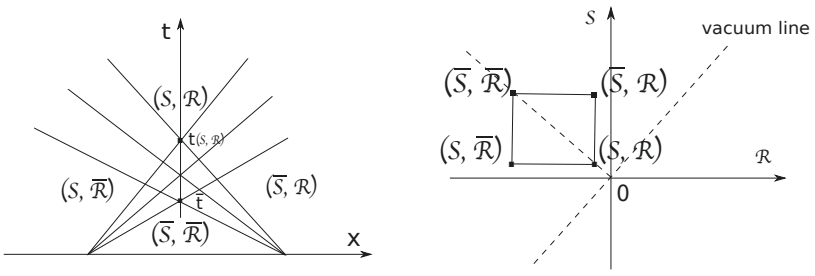


FIGURE 1. Interaction of two centered rarefaction waves.

where $t(\mathcal{S}, \mathcal{R})$ is the time when the interaction ends, $F(z_1, z_2, z_3, z_4)$ is a hypergeometric function and

$$\sigma = \frac{\gamma + 1}{2(\gamma - 1)}. \tag{9}$$

When $\sigma$ is a positive integer $N$ or equivalently

$$\gamma = \frac{2N + 1}{2N - 1},$$

the equation (8) is reduced into

$$t(\mathcal{S}, \mathcal{R}) = \bar{t} \left( \frac{\bar{\mathcal{S}} - \bar{\mathcal{R}}}{\mathcal{S} - \mathcal{R}} \right)^{\sigma} P_{\sigma-1} \left( \frac{1}{\bar{\mathcal{S}}} \frac{\bar{\mathcal{S}}^2 - \mathcal{S}\mathcal{R}}{\mathcal{S} - \mathcal{R}} \right), \tag{10}$$

where $P_{\sigma-1}(z)$ is the Legendre's function, which is a $(\sigma - 1)$-th order polynomial.

Recall that we assume that $\mathcal{S}$ in the left state of interaction is always positive and $\mathcal{R}$ in the right state of interaction is always negative. Let $|\mathcal{S}|$ and $|\mathcal{R}|$ be both very small, then density $\rho$ at the point where interaction ends (at time $t(\mathcal{S}, \mathcal{R})$) is very close to zero. Using (7), to the leading order, we have

$$t(\mathcal{S}, \mathcal{R}) = O(\rho^{-1}),$$

where we used (6), (9)-(10), $P_{\sigma-1}(z)$ is a $(\sigma - 1)$-th order polynomial and $\frac{1}{\bar{\mathcal{S}}}(\bar{\mathcal{S}}^2 - \mathcal{S}\mathcal{R}) > \bar{\mathcal{S}}$ is uniformly positive. When $|\mathcal{S}|$ and $|\mathcal{R}|$ both approach zero,

$$t(\mathcal{S}, \mathcal{R}) \to \infty.$$

So when $t$ is large enough,

$$\min_x \rho(x, t) = O(1 + t)^{-1}.$$

It is clear that the initial density in this explicit example is uniformly positive, as illustrated in the right picture of Figure 1.

For general $\gamma > 1$, similar calculation on the density lower bound for the interaction of centered rarefactions can be found in [14].

3. **The polygonal scheme and Rarefaction/Compression character.** In this section, we review some basic setup for the polygonal scheme following the notations in [17, 19]. Here, we adapt a simpler version of the scheme used in [19].

3.1. **Pressure, Riemann invariants and Standard states.** We first give the polygonal approximation of $p(v)$ as follows: for any given positive integer $n$, let $v_0^{(n)} = 1$, and $v_k^{(n)}$ (for integer $k$) be determined by the recurrence formula

$$G(v_k^{(n)}, v_{k+1}^{(n)}) := \Big(p(v_k^{(n)}) - p(v_{k+1}^{(n)})\Big)\Big(v_{k+1}^{(n)} - v_k^{(n)}\Big) = \frac{1}{n^2}\,. \tag{11}$$

It is easy to check that for each fixed $n$ there exists a unique sequence $\Big\{v_k^{(n)}\Big\}_{k=1}^{\infty}$, defined by (11), such that

$$\lim_{k\to\infty} v_k^{(n)} = \infty, \quad \text{and} \quad \lim_{k\to-\infty} v_k^{(n)} = 0\,.$$

Furthermore, denoting

$$\delta_k^{(n)} := v_{k+1}^{(n)} - v_k^{(n)}\,,$$

one has

$$\lim_{k\to\infty} \delta_k^{(n)} = \infty\,.$$

By connecting the points $\big(v_k^{(n)},\, p(v_k^{(n)})\big)$ and $\big(v_{k+1}^{(n)},\, p(v_{k+1}^{(n)})\big)$ through straight lines, we have a polygonal approximation for $p(v)$, denoted by $p^{(n)}(v)$.

In the second step, based on the definition of $p^{(n)}(v)$, we give the polygonal approximation of Riemann invariants $r$ and $s$. Denoting

$$\Phi^{(n)}(v) := \int_1^v \sqrt{-{p^{(n)}}'(v)}\, dv\,, \tag{12}$$

then

$$\Phi^{(n)}(v_0^{(n)}) = \Phi^{(n)}(1) = 0\,,$$

and

$$\Phi^{(n)}(v_{k+1}^{(n)}) - \Phi^{(n)}(v_k^{(n)}) = \sqrt{G(v_k^{(n)}, v_{k+1}^{(n)})} = \frac{1}{n}\,.$$

One quickly has

$$\Phi^{(n)}(v_k^{(n)}) = \frac{k}{n}\,,$$

where $k$ is an integer and $n$ is a positive integer.

We define

$$r^{(n)}(u,v) = u + \Phi^{(n)}(v), \qquad s^{(n)}(u,v) = u - \Phi^{(n)}(v)\,, \tag{13}$$

which are corresponding to the Riemann invariants $r$ and $s$ defined in (3), respectively.

Finally, we give the definition of standard states:

$$\big(u,\, v\big) = \Big(\frac{i}{n},\, v_j^{(n)}\Big), \quad i.e. \quad \big(u,\, \Phi^{(n)}\big) = \Big(\frac{i}{n},\, \frac{j}{n}\Big)\,,$$

and

$$\big(r^{(n)},\, s^{(n)}\big) = \Big(\frac{2k}{n},\, \frac{2l}{n}\Big)\,,$$

where $i$ and $j$ are integers satisfying

$$k = \frac{1}{2}(i+j) \quad \text{and} \quad l = \frac{1}{2}(i-j)\,.$$

For convenience, we might omit the superscript $(n)$ if there are no confusions.

3.2. **Riemann problems.** Based on the definitions introduced in the previous subsection, now we consider the following Riemann problem:

$$\begin{cases} v_t - u_x &= 0\,, \\ u_t + p^{(n)}(v)_x &= 0\,, \\ \big(u_0(x),\, v_0(x)\big) &= \begin{cases} \big(u_-,\, v_-\big), & x<0\,, \\ \big(u_+,\, v_+\big), & x>0\,, \end{cases} \end{cases} \tag{14}$$

with

$$\big(u_-,\, v_-\big) = \Big(\frac{i}{n},\, v_j^{(n)}\Big)\,, \qquad \big(u_+,\, v_+\big) = \Big(\frac{i+M+N}{n},\, v_{j+M-N}^{(n)}\Big)\,,$$

where $M$ (and $N$) can be $-1$, 0 or 1. Clearly, we have

$$\big(r_0^{(n)}(x),\, s_0^{(n)}(x)\big) = \begin{cases} \big(r_-^{(n)},\, s_-^{(n)}\big), & x<0\,, \\ \big(r_+^{(n)},\, s_+^{(n)}\big), & x>0\,, \end{cases}$$

with

$$\big(r_-^{(n)},\, s_-^{(n)}\big) = \Big(\frac{2k}{n},\, \frac{2l}{n}\Big)\,, \qquad \big(r_+^{(n)},\, s_+^{(n)}\big) = \Big(\frac{2(k+M)}{n},\, \frac{2(l+N)}{n}\Big)\,.$$

The solution of the Riemann problem (14) consists of $|M|+|N|+1$ standard states, divided by $|M|+|N|$ jump discontinuities (straight lines centered at the origin).

To calculate the middle state $(r_m^{(n)}, s_m^{(n)})$ in the solution of Riemann problem (14), we use the following criterions:

$$s^{(n)} \quad \text{and} \quad r^{(n)} \quad \text{are constants across backward and forward jumps, respectively.} \tag{15}$$

This criterion follows from (3). Hence the middle state in the solution of Riemann problem (14) is always

$$\big(r_m^{(n)}, s_m^{(n)}\big) = \Big(\frac{2(k+M)}{n}, \frac{2l}{n}\Big).$$

Then it is easy to have

$$\big(u_m, v_m\big) = \Big(\frac{i+M}{n},\, v_{j+M}^{(n)}\Big).$$

**Remark 1.** We note that

- if $M=1$ (resp. $N=1$), the backward (resp. forward) jump discontinuity describes a rarefactive wave.
- If $M=0$ (resp. $N=0$), there are no backward (resp. forward) jump discontinuity.
- if $M=-1$ (resp. $N=-1$), the backward (resp. forward) jump discontinuity describes a compressive wave.

The definitions of rarefaction and compression are in Definition 1.1. We refer the readers to [2, 5] for more details on wave curves for rarefaction and compression waves.

When $M$ is $-1$ or 1, from (11), the slope of the backward jump is

$$\overleftarrow{\lambda} = -\sqrt{-\frac{p(v_{j+M}^{(n)}) - p(v_j^{(n)})}{v_{j+M}^{(n)} - v_j^{(n)}}} = \frac{-1}{n\left|v_{j+M}^{(n)} - v_j^{(n)}\right|} < 0. \tag{16}$$

When $N$ is $-1$ or 1, from (11), the slope of the forward jump is

$$\overrightarrow{\lambda} = \sqrt{-\frac{p(v_{j+M}^{(n)}) - p(v_{j+M-N}^{(n)})}{v_{j+M}^{(n)} - v_{j+M-N}^{(n)}}} = \frac{1}{n\left|v_{j+M}^{(n)} - v_{j+M-N}^{(n)}\right|} > 0. \tag{17}$$

3.3. **The polygonal scheme and Rarefactive/Compressive characters.** For any given Lipschitz continuous initial data $(r_0, s_0)$ with $u_0$ and $v_0$ uniformly bounded and $v_0$ uniformly away from zero, similar to [17], we can find a sequence of piecewise constant functions $(u_0^{(n)}, v_0^{(n)})$ which takes values on finitely many standard states. More precisely, for arbitrary integer $n > 0$, there exist finite points $-\infty = x_1^{(n)} < x_2^{(n)} < ... < x_j^{(n)} < x_{j+1}^{(n)} = +\infty$, such that for every integer $1 \le \alpha \le j$,

$$\left(r^{(n)}(x),\, s^{(n)}(x)\right) = \left(\frac{2k_\alpha^{(n)}}{n},\, \frac{2l_\alpha^{(n)}}{n}\right),$$

for some integers $k_\alpha^{(n)}$ and $l_\alpha^{(n)}$ for $x \in (x_\alpha^{(n)}, x_{\alpha+1}^{(n)})$.

Furthermore, $(k_{\alpha-1}^{(n)}, l_{\alpha-1}^{(n)})$ is different from $(k_\alpha^{(n)}, l_\alpha^{(n)})$ and

$$|k_{\alpha-1}^{(n)} - k_\alpha^{(n)}| \le 1, \qquad |l_{\alpha-1}^{(n)} - l_\alpha^{(n)}| \le 1\,.$$

For such sequence, we have

$$(u_0^{(n)}, v_0^{(n)}) \to (u_0, v_0) \tag{18}$$

uniformly, and

$$\max_\alpha \frac{2}{n\left(x_{\alpha+1}^{(n)} - x_\alpha^{(n)}\right)} \longrightarrow \max_{x \neq y}\left\{\frac{s_0(x) - s_0(y)}{x - y}, \frac{r_0(x) - r_0(y)}{x - y}\right\}, \quad \text{as} \quad n \to \infty\,. \tag{19}$$

Here, in fact, we can choose the approximation piecewise constant profiles of $s^{(n)}(x)$ and $r^{(n)}(x)$ such that when $x$ is varying from $x_\alpha$ to $x_{\alpha+1}$, the variations of $s$ and $r$ values are equal to $\pm\frac{2}{n}$, which more precisely means,

$$s^{(n)}(x_{\alpha+1} + \varepsilon) - s^{(n)}(x_\alpha + \varepsilon) = \pm\frac{2}{n} \quad \text{and} \quad r^{(n)}(x_{\alpha+1} + \varepsilon) - r^{(n)}(x_\alpha + \varepsilon) = \pm\frac{2}{n}$$

when $\varepsilon$ is small enough. So as $n \to \infty$, (19) is satisfied.

For any positive integer $n$, we solve the Riemann problem (14) at each discontinuity. Note the left, right and middle sates in the solution of each Riemann problem (14) are still standard states, split by jump discontinuities. Let these jump discontinuities evolve. When two jumps in different characteristic families interact with each other, new Riemann problem appears, which can also be solved according to the method established in the previous subsection and there are exactly two outgoing jumps. Before the possible interactions between jumps of the same family, we get a well-defined polygonal scheme, including finitely many jumps, because the total number of interactions are finite and the number of outgoing discontinuities equals to the number of incoming discontinuities in one interaction.

In [19], the authors show that under some regularity condition on the initial data $(u_0, v_0)$, the approximation solutions $(u^{(n)}, v^{(n)})$ in the polygonal scheme used in current paper are well-defined, i.e. there is no interaction between jumps of the same family, in a time interval $t \in [0, T]$ with $T > 0$ only dependent on the $C^1$-norm of $(u_0, v_0)$ but independent of $n$. Furthermore, the approximation solutions converge to a Lipschitz continuous solution for p-system when $n \to \infty$. We will give more details on this local-in-time convergence result later.

In this subsection, we first assume that there is no interaction between jumps of the same family.

**Definition 3.1.** In the polygonal scheme, for any positive integer $n$, the $(x, t)$-plane is divided into finite *blocks* by finitely many jump discontinuities. If a block is a diamond, we call it a *diamond block* or *diamond*. Each jump discontinuity may also be divided into finite many pieces, which are denoted by *jump edges*, by finitely many intersection points with other jumps.

To be precise on the definitions of a block or a jump edge, we note $s^{(n)}$ and $r^{(n)}$ are both constants inside each block and on each side of a jump edge, or in another word, there are no other jump discontinuities going inside a block or a jump edge.

To obtain a good lower bound on density, it is crucial to study the variation of a jump edge inside a characteristic tube, such as the propagation of edge $l_1$ in the forward characteristic direction in Figure 2.

First, we define the Rarefactive/Compressive (R/C) character on a jump edge.

**Definition 3.2** (R/C character on a jump edge)**.** We classify the jump edges into four types: $R_r$, $R_c$, $C_r$ and $C_c$. Most of time, we add an arrow to denote forward or backward character, respectively.

More precisely, a backward (resp. forward) jump edge $l_1$ (resp. $l_2$) in the scheme, shown in Figure 2, is said to be:

i. $\overrightarrow{R}_r$ (resp. $\overleftarrow{R}_r$), if $u_- < u_+ < u_{++}$ (resp. $u_{--} < u_- < u_+$).
ii. $\overrightarrow{R}_c$ (resp. $\overleftarrow{R}_c$), if $u_- < u_+$ and $u_+ > u_{++}$ (resp. $u_- < u_+$ and $u_{--} > u_-$).
iii. $\overrightarrow{C}_r$ (resp. $\overleftarrow{C}_r$), if $u_- > u_+$ and $u_+ < u_{++}$ (resp. $u_- > u_+$ and $u_{--} < u_-$).
iv. $\overrightarrow{C}_c$ (resp. $\overleftarrow{C}_c$), if $u_- > u_+ > u_{++}$ (resp. $u_{--} > u_- > u_+$).

For the left-most forward (resp. right-most backward) jump edge in the scheme which is unbounded from its left (resp. right) hand side, we always say this jump edge belongs to either $C_c$ or $R_r$ by checking the relation of $u$ from the right (resp. left) boundary following the table above.

For simplicity, we always use $C$ to denote $C_r$ or $C_c$ character.

**Remark 2.** In the definition of $R_r$, $R_c$, $C_r$ and $C_c$, the capital letter denotes the character on the boundary behind the edge ($u$ increases from left to right for a rarefaction boundary) and the subscript denotes character on the boundary ahead of the edge.

In Figure 2, we use the subscripts $a$ and $b$ to denote states ahead of and behind a jump wave front. By (15), one always has $v_b > v_a$ for a $R_r$ or $R_c$ jump edge; and $v_b < v_a$ for a $C_r$ or $C_c$ jump edge. In the $R_c$ and $C_r$ pieces, $v_{aa} = v_b$.

Then we define the $R/C$ character on any blocks.

**Definition 3.3** (R/C character in a block)**.** A block is called a $\overrightarrow{R}_r\overleftarrow{R}_r$ block if its South-West and South-East boundaries are $\overrightarrow{R}_r$ and $\overleftarrow{R}_r$, respectively.

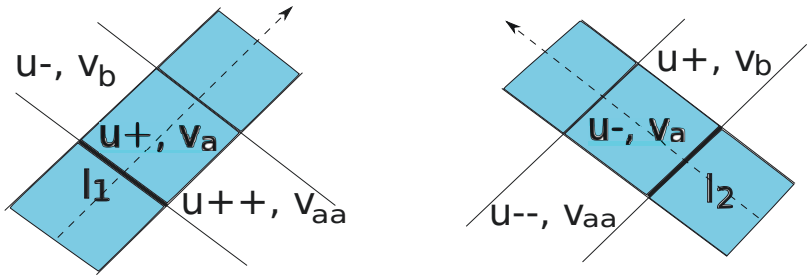


FIGURE 2. Definition of forward (resp. backward) R/C characters for the jump edge $l_1$ (resp. $l_2$). The picture is on the $(x,t)$-plane.

Similar definitions are also for $\overrightarrow{R}_r\overleftarrow{R}_c$ $\overrightarrow{R}_c\overleftarrow{R}_r$, $\overrightarrow{R}_c\overleftarrow{R}_c$, $\overrightarrow{C}\overleftarrow{R}_r$, $\overrightarrow{C}\overleftarrow{R}_c$, $\overrightarrow{R}_r\overleftarrow{C}$, $\overrightarrow{R}_c\overleftarrow{C}$ and $\overrightarrow{C}\overleftarrow{C}$ blocks.

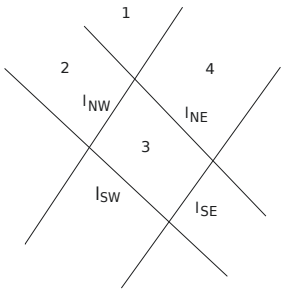


FIGURE 3. Proof of Lemma 3.4. The picture is on the $(x,t)$-plane.

**Lemma 3.4.** *The forward (resp. backward) jump edges $l_{SW}$ and $l_{NE}$ (resp. $l_{SE}$ and $l_{NW}$) shown in Figure 3 belong to the same type.*

*Proof.* By (13) and (15), we have

$$u_1^{(n)} - u_4^{(n)} = \Phi_4^{(n)} - \Phi_1^{(n)}, \quad u_3^{(n)} - u_2^{(n)} = \Phi_2^{(n)} - \Phi_3^{(n)},$$

and

$$u_1^{(n)} - u_2^{(n)} = \Phi_1^{(n)} - \Phi_2^{(n)}, \quad u_3^{(n)} - u_4^{(n)} = \Phi_3^{(n)} - \Phi_4^{(n)}.$$

Summing up these equations, one obtains

$$u_1^{(n)} - u_2^{(n)} = u_4^{(n)} - u_3^{(n)} \quad \text{and} \quad u_1^{(n)} - u_4^{(n)} = u_2^{(n)} - u_3^{(n)}, \tag{20}$$

with states 1∼4 given in Figure 3, hence the monotonicity of $u$ is preserved in both forward and backward directions, which is enough to prove this lemma by Definition 3.2. □

**Definition 3.5** (R/C character in a district)**.** Given a block in certain type (for example a $\overrightarrow{R}_r\overleftarrow{R}_r$ block), we define a *district* in that type (for example a $\overrightarrow{R}_r\overleftarrow{R}_r$ district) to be the largest connected set which includes the given block and consists of only blocks in the same type.

Finally, we prove that $v$ decays in some direction, when we restrict our consideration on districts which are not in $\overrightarrow{R}_r\overleftarrow{R}_r$ type.

**Lemma 3.6.** *If the forward character of a district $D$ is $\overrightarrow{C}$ or $\overrightarrow{R}_c$, then $v$ on any block adjacent to and above North-West boundary of $D$ is not larger than the maximum $v$ values on blocks adjacent and below South-East boundary of $D$.*

*And all $\Phi^{(n)}$ values on blocks in $D$ are at most $1/n$ larger than the maximum $\Phi^{(n)}$ value on blocks adjacent and below South-East boundary of $D$.*

*Symmetric decay of $v$ happens if the backward character of a district $D$ is $\overleftarrow{C}$ or $\overleftarrow{R}_c$.*

The proof of this lemma is obvious from Remark 2. This lemma is corresponding to the fact that density increases from behind to ahead of a compression simple wave.

4. **The lower bound on density in the scheme.** This section will be devoted to prove density's lower bound estimate shown in Theorem 1.2. The key idea in proving (5) is to define a function $a^{(n)}(t)$ for any $n$, which is not decreasing on $t$. The monotonicity of $a^{(n)}(t)$ will finally lead to a lower bound on density, under the help of the local convergence theorem for the polygonal scheme in [19]. In this section, we always assume that jumps in the same family do not interact, where this assumption will be removed in the end of this section.

To define $a^{(n)}(0)$, in the first step, we modify some blocks adjacent to the initial line $t = 0$ to diamonds, as in Figure 4 and the left picture of Figure 5. After these modifications, we call all interior and boundary diamonds as complete diamonds, also shown in Figure 4.

**Definition 4.1.** Call the collection of all complete diamonds (after modifications) as $\mathcal{CD}$. The lowest boundary of $\mathcal{CD}$ is a polygonal line, denoted by $t = L_0^{(n)}(x)$. It is clear that $t = L_0^{(n)}(x)$ consists of finitely many jump edges. See Figure 5.

A jump edge $JE_i$ on $t = L_0^{(n)}(x)$ is said in $L_{0,R}^{(n)}$ if it is $\overrightarrow{R}_r$ or $\overleftarrow{R}_r$. We define the length of the propagation of $JE_i$ onto $x$-axis as $a_i^{(n)}(0)$. Now we define

$$a^{(n)}(0) = \min_{JE_i \in L_{0,R}^{(n)}} a_i^{(n)}(0)\,.$$

For $t > 0$, it is not necessary to modify the diamond again. We thus define $a^{(n)}(t)$ in a similar way.

We first give a lemma on the initial data.

**Lemma 4.2.** *Assume the initial density $\rho^{(n)}(x, 0)$ has positive upper and lower bounds, and*

$$J = \max_{x \neq y} \left\{ \frac{s_0(x) - s_0(y)}{x - y}, \frac{r_0(x) - r_0(y)}{x - y} \right\} < \infty, \tag{21}$$

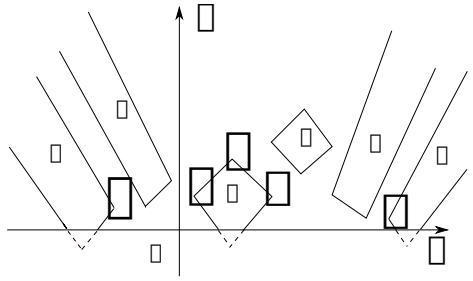

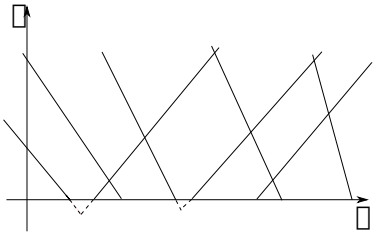

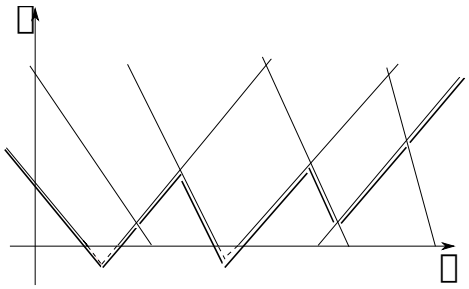

*then the density* $\rho^{(n)}\big(x, L_0^{(n)}(x)+\big)$ *has positive lower and upper bounds. And*

$$\lim_{n\to\infty} \frac{1}{n\, a^{(n)}(0)} \le M_0 J\,, \tag{22}$$

*and* $M_0$ *is a positive constant depending on the uniform upper and lower bound on initial density but independent of* $n$*.*

**Remark 3.** By (18), we know that, under the assumptions on initial data in Theorem 1.2, assumptions in Lemma 4.2 are all satisfied. $M_0$ only depends on $L_3$ and $L_4$, by the definition of $s$ and $r$ in (2)∼(4). $J$ clearly only depends on $L_1$ and $L_2$. The definition of $L_1$∼$L_4$ are given in Theorem 1.2.

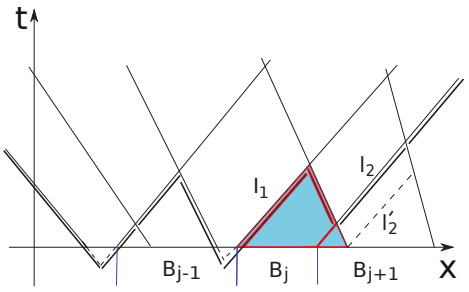


FIGURE 6. Proof of Lemma 4.2. $l_2$ and $l_2'$ are parallel with each other. The picture is on the $(x,t)$-plane.

*Proof.* The first claim is clearly true because each state below the curve $t = L_0(x)$ is an initial state in the scheme.

To prove (22), it is enough to show that for any jump edge $PQ$ with endpoints $P$ and $Q$ on the curve $t = L_0^{(n)}(x)$, we have

$$\frac{1}{n|x_P - x_Q|} \le M_0 J + \varepsilon_n, \tag{23}$$

where $\varepsilon_n$ goes to zero as $n$ goes to infinity.

We divide jump edges on the curve $t = L_0^{(n)}(x)$ into two types: jump edge intersecting with the initial line and jump edge not intersecting with the initial line. Without loss of generality, we only consider two forward jump edges $l_1$ and $l_2$ in Figure 6.

We denote three line segments on $t = 0$ divided by adjacent backward jumps as $B_{j-1}$, $B_j$ and $B_{j+1}$, respectively, which are shown in Figure 6.

Noticing that $l_1$ is $\overleftarrow{R}_r$, from (15), Definition 3.2 and the discussion in Subsection 3.1, we have $r = \frac{2(k-1)}{n}$, $\frac{2k}{n}$ and $\frac{2(k+1)}{n}$ in backward tubes, which means that all connected blocks are divided by two adjacent backward jumps, including $B_{j-1}$, $B_j$ and $B_{j+1}$, respectively, where $k = \frac{1}{2}(i+j)$ for some integers $i$ and $j$.

By studying the shaded triangle in Figure 6, it is easy to get that there exists a constant $M$ only depending on the upper and lower bounds of initial density, such that

$$M \geq \frac{|B_j|}{\Delta_{l_1} x}$$

as $n$ large enough, where $\Delta_{l_1} x$ means the length of projection of $l_1$ onto the line $t = 0$. Then we have

$$\frac{\frac{2}{n}}{\Delta_{l_1} x} \leq M \frac{r_{B_{j+1}} - r_{B_{j-1}}}{|B_j|}. \tag{24}$$

Hence (23) is clearly correct, because the right hand side of (24) is bounded above by $J$ as $n$ goes to infinity, where we have also used (19).

For $l_2$, noting that $\Delta_{l_2} x \geq \Delta_{l_2'} x$ where $l_2'$ is parallel to $l_2$, because $l_2$ is $\overleftarrow{R}_i$, we know that two backward jumps enclosing $l_2$ open up. A more detailed argument on this fact can be found in Step 2.1 in the proof of Lemma 4.3. Now we change the problem to a problem for $l_2'$ which intersects with $t = 0$, hence similar as the case for $l_1$, we can prove (23).

This completes the proof of the lemma. □

The following lemma plays a key role in this paper.

**Lemma 4.3.** *Assume all assumptions on initial data in Theorem 1.2 hold. For any positive time $T$, suppose the scheme is well-defined on $\mathbb{R} \times [0, T]$, then $a^{(n)}(t)$ is not decreasing on $t$ for all $t \in [0, T]$.*

*Proof.* We divide our proof into two steps. For convenience, we omit the subscript $(n)$ in the proof of this lemma.

**Step 1.** Suppose jump edges $P_u P_l$ and $P_{u'} P_l$ are two lower boundaries of a diamond $\Omega$, where $P_u$, $P_{u'}$ and $P_l$ are three vertexes of $\Omega$, and specially $P_l$ is the lowest vertex.

Then we prove that: for any time $T \geq 0$, $P_u P_l$ and $P_{u'} P_l$ are either **both in** or **both not in** the collection of selected diamonds at time $T$.

Actually, if $P_l$ is in the region $t \geq T$, then $\Omega$ is a selected diamond.

If $P_l$ is not in the region $t \geq T$, then diamonds containing $P_u P_l$ or $P_{u'} P_l$ as north boundary are not selected. Thus except these diamonds, the only diamond including $P_u P_l$ or $P_{u'} P_l$ is $\Omega$. Hence $P_u P_l$ and $P_{u'} P_l$ are either both selected or both not selected.

**Step 2.** Recall that the R/C characteristic does not change along forward and backward characteristic directions. Also using the claim proved in Step 1, to prove the lemma, we only have to show that, in any diamond, the minimum difference in $x$ for any $\overrightarrow{R}_r$ and $\overleftarrow{R}_r$ south jump edges is less or equal to the minimum difference in $x$ for any $\overrightarrow{R}_r$ and $\overleftarrow{R}_r$ north jump edges.

We discuss case by case for diamonds including $\overrightarrow{R}_r$ or $\overleftarrow{R}_r$.

**Case (2.1).** We consider a $\overrightarrow{R}_r \overleftarrow{C}$ or a $\overrightarrow{R}_r \overleftarrow{R}_c$ diamond shown in Figure 7. We use subscripts $E$, $W$, $N$ and $S$ to denote functions related to east, west, north and south endpoints of the diamond, respectively. And we use subscripts $NE$, $NW$, $SE$ and $SW$ to denote functions related to North-East, North-West, South-East

and South-West boundary jump edges of the diamond, respectively. Especially we use $l_{NE}$, $l_{NW}$, $l_{SE}$ and $l_{SW}$ to denote the North-East, North-West, South-East and South-West boundary jump edges of the diamond.

We want to show that

$$x_E - x_N \geq x_S - x_W. \tag{25}$$

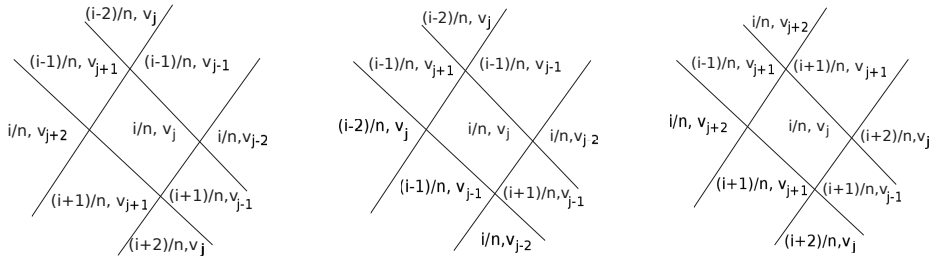


FIGURE 7. From left to right: the middle diamonds are: $R_rC_c$; $R_rC_r$; and $R_rR_c$ diamonds, respectively, where forward character always goes first. The picture $(x,t)$-plane.

By studying the three possible cases in Figure 7 using (16)$\sim$(17), we always have

$$0 < \frac{\lambda_{NW}}{\lambda_{SE}} < 1 \quad \text{and} \quad 1 \leq \frac{\lambda_{NE}}{\lambda_{SW}}, \tag{26}$$

where recall that subscripts $N$, $S$, $W$, $E$ denote the north, south, west and east endpoints of the middle diamond in the figure, respectively.

Then we could give an easy geometric proof for (25) in Figure 8. In fact, drawing two dash lines parallel to $l_{NW}$ and $l_{SW}$, respectively, then by (26), we know the parallelogram is inside the diamond, although in $\overline{R}_r\overline{C}_r$ and $\overline{R}_r\overline{R}_c$ diamonds in Figure 7 one edge of the parallelogram lies on $l_{NE}$. Then by Figure 8, clearly (25) is correct.

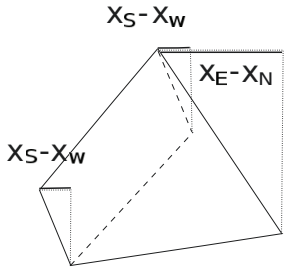


FIGURE 8. The proof of (25) on a diamond satisfying (26). The picture is on the $(x,t)$-plane.

**Case (2.2).** However, the easy geometric proof in the previous part fails for $\overrightarrow{R}_r\overleftarrow{R}_r$ interaction where the second inequality in (26) is in the opposite direction. Instead we use the similar idea as the one used in [17] to cope with a $\overrightarrow{R}_r\overleftarrow{R}_r$ diamond.

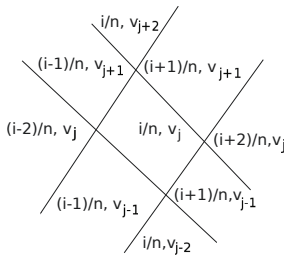


FIGURE 9. The center diamond is a $R_rR_r$ block. The picture is on the $(x,t)$-plane.

We use $B$ and $D$ to denote the difference in $x$ and $t$ for each adjacent pair of endpoints on the diamond, respectively, such as

$$B_{NW} = |x_N - x_W|, \qquad D_{NW} = |t_N - t_W|. \tag{27}$$

Then clearly one has

$$B_{NW} + B_{NE} = B_{SW} + B_{SE},$$
$$D_{NW} + D_{SW} = D_{NE} + D_{SE},$$

and

$$\frac{B_{NW}}{D_{NW}} = \frac{B_{NE}}{D_{NE}} = \lambda_{NW} < \lambda_{SE} = \frac{B_{SW}}{D_{SW}} = \frac{B_{SE}}{D_{SE}}.$$

Denote that

$$0 < \alpha = \frac{\lambda_{NW}}{\lambda_{SE}} < 1,$$

it is easy to deduce that

$$B_{NW} = \frac{1}{2}(1+\alpha)B_{SE} + \frac{1}{2}(1-\alpha)B_{SW},$$

and

$$B_{NE} = \frac{1}{2}(1+\alpha)B_{SW} + \frac{1}{2}(1-\alpha)B_{SE}.$$

Hence we have

$$\min(B_{NW}, B_{NE}) > \min(B_{SW}, B_{SE}), \tag{28}$$

which is the estimate we need.

Combining all the information obtained above, we have finished the proof of this lemma. □

Finally we prove Theorem 1.2.

*Proof.* We divide our proof into two steps.

**Step 1.** First we show that: Suppose the polygonal scheme is well-defined when $0 < t \le T^*$. Then we have, when $n$ is sufficiently large,

$$v^{(n)}(x,t) \le \max_x v_0^{(n)}(x) + L \cdot t \quad \text{when} \quad 0 < t \le T^* \tag{29}$$

for a uniform constant $L = L(L_1, L_2, L_3, L_4)$ independent of $n$, where constants $L_1 \sim L_4$ are defined in Theorem 1.2.

By Lemma 3.6, we know that $v^{(n)}$ is not increasing along some direction in any districts except $\overrightarrow{R}_r\overleftarrow{R}_r$ districts. Hence in these districts clearly we have

$$\max_{\text{in whole district}} \Phi(v^{(n)}) \le \max_{\text{on lower boundary of the district}} \Phi(v^{(n)}) + \frac{1}{n}. \tag{30}$$

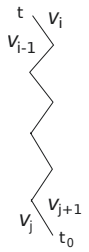


FIGURE 10. Bound on $v^{(n)}$ in a $R_rR_r$ district. In the figure, we omit the subscript $(n)$ for convenience. The picture is on the $(x,t)$-plane.

Next, in the $\overrightarrow{R}_r\overleftarrow{R}_r$ district, we will use the result obtained in Lemma 4.3 that $a^{(n)}(t)$ is not decreasing on $t$ to prove (29). To see it, choose a block with $v = v_i^{(n)}(t)$ inside this block, then trace it back to a block with $v = v_j^{(n)}(t_0)$ on the lower boundary of the considered $\overrightarrow{R}_r\overleftarrow{R}_r$ district by a series of jump edge shown in Figure 10. The $v$ values in Figure 10 are given according to a fact that in the $\overrightarrow{R}_r\overleftarrow{R}_r$ district if $v^{(n)} = v_k^{(n)}$ ahead of a jump edge then $v^{(n)} = v_{k+1}^{(n)}$ behind that jump edge. Then by (16)$\sim$(17) and the definition of $a^{(n)}(t)$, we have

$$t - t_0 \ge a^{(n)}(0) \sum_{k=j}^{i} n(v_{k+1}^{(n)} - v_k) = na^{(n)}(0)(v_i^{(n)} - v_j^{(n)}),$$

which immediately implies that

$$v_i^{(n)} \le v_j^{(n)} + \frac{1}{na^{(n)}(0)}(t - t_0)\,. \tag{31}$$

Then using Lemma 4.2, Remark 3, (30) and (31), we can prove (29), where note for each polygonal scheme, there are at most finitely many districts.

**Step 2.** The local-in-time existence result in [19] shows that under the assumption in Theorem 1.2, there exists a time interval $t \in [0, \varepsilon]$ in which the polygonal schemes are well-defined when $n$ is sufficiently large and converging to a Lipschitz continuous solution for (1) as $n$ approaches infinity. The constant $\varepsilon$ is only dependent of Lipschitz norms on $v$ and $u$, but independent of $n$.

By the weak-strong uniqueness of the classical solution for (1), c.f. [10], we know the Lipschitz continuous solution of (1) when $t \in [0, \varepsilon]$ agrees with the solution

through the limit of polygonal scheme. Hence any Lipschitz continuous solution satisfies (5) by the a priori estimate in (29) for the approximation solution.

Then, for any finite time $T > 0$ and any Lipschitz continuous solutions on $[0, T]$, repeating above process finite many times, we prove that the solution always satisfies (5) when $t \in [0, T]$, where in each time we could evolve by a time step $\varepsilon$ which is constant. This completes the proof of the theorem. □

5. **Life span of classical solutions.** In this section, we apply the time-dependent lower bound (5) obtained in Theorem 1.2 to achieve a better estimate for the life-span of classical solutions including compression than [7], when $1 < \gamma < 3$. Before stating this result, we first review a lemma coming from [7, 15].

**Lemma 5.1.** [7, 15] *For $C^1$ solutions of (1) we have*

$$\partial_+ y = -K_0 v^{\frac{\gamma-3}{4}} y^2 , \tag{32}$$

$$\partial_- q = -K_0 v^{\frac{\gamma-3}{4}} q^2 , \tag{33}$$

*where*

$$y(x,t) := \sqrt{c}\, s_x, \qquad q(x,t) := \sqrt{c}\, r_x$$

*and $K_0$ is a constant only depending on $\gamma$ which can be easily found in* [7].

Then the estimates on the life-span of classical solutions including compression can be given in the following corollary.

**Corollary 1.** *Assume all assumptions in Theorem 1.2 hold, the initial data $s_0(x)$ and $r_0(x)$ are $C^1$, and*

$$G_0 := \min_x \big(y(x,0), q(x,0)\big) < 0, \tag{34}$$

*i.e. the initial data are compressive somewhere, then singularity happens not later than*

$$t = \frac{1}{L}\left\{ \Big( -\frac{4K_0}{\gamma+1}\frac{1}{G_0} + H_0^{\frac{\gamma+1}{4}} \Big)^{\frac{4}{\gamma+1}} - H_0 \right\} ,$$

*where we denote*

$$H_0 := \max_x v(x,0) .$$

*Proof.* Without loss of generality, we assume that

$$y(x^*,0) = G_0 + \varepsilon = \min_x \big(y(x,0), q(x,0)\big) + \varepsilon < 0,$$

where $0 < \varepsilon \ll 1$ is a constant.

For smooth solutions, along a forward characteristic $x^+(t)$ starting from $(x^*, 0)$, by (32), one has

$$\frac{1}{y\big(x^+(t),t\big)} = \frac{1}{y\big(x^*,0\big)} + \int_0^t K_0 v^{\frac{\gamma-3}{4}}\big(x^+(\xi),\xi\big) d\xi .$$

Then the right hand side of this equation equals to zero, i.e. $y\big(x^+(t),t\big)$ blows up, not later than a time $t$ satisfying

$$-\frac{1}{y\big(x^*,0\big)} = \int_0^t K_0 v^{\frac{\gamma-3}{4}}\big(x^+(\xi),\xi\big) d\xi .$$

Thus by (5) in Theorem 1.2, it is very easy to finish the proof of this corollary, where we use that $\varepsilon$ can be arbitrarily small. □

**REFERENCES.**


[1] A. Bressan, *Hyperbolic systems of conservation laws: the 1-dimensional Cauchy problem*, Oxford Univ. Press, Oxford 2000.

[2] A. Bressan, G. Chen, and Q. Zhang, Lack of BV bounds for approximate solutions to the $p$-system with large data, *J. Differential Equations*, **256**: 8 (2014), 3067–3085.

[3] T. Chang and L. Hsiao, *The Riemann problem and interaction of waves in gas dynamics*, Pitman Monographs and Surveys in Pure and Applied Mathematics, **41**,Longman Scientific & Technical, Harlow; copublished in the United States with John Wiley & Sons, Inc., New York, 1989.

[4] G. Chen, Formation of singularity and smooth wave propagation for the non-isentropic compressible Euler equations, *J. Hyperbolic Differ. Equ.*, **8**:4 (2011), 671-690.

[5] G. Chen and H. K. Jenssen, No TVD fields for 1-D isentropic gas flow, *Comm. Partial Differential Equations*, **38**:4 (2013), 629–657.

[6] G. Chen, R. Young and Q. Zhang, Shock formation in the compressible Euler equations and related systems, *J. Hyperbolic Differ. Equ.*, **10**:1 (2013), 149-172.

[7] G. Chen, R. Pan and S. Zhu, Singularity formation for the compressible Euler equations, *SIAM J. Math. Anal.*, **49** : 4, (2017), 2591–2614.

[8] G. Chen and R. Young, Shock formation and exact solutions for the compressible Euler equation, *Arch. Rational Mech. Anal.*, **217**, (2015), 1265–1293,

[9] R. Courant and K. O. Friedrichs, *Supersonic flow and shock waves*, Wiley-Interscience, New York, 1948.

[10] C. M. Dafermos, *Hyperbolic conservation laws in continuum physics*, Third edition, Springer-Verlag, Heidelberg, 2010.

[11] C. M. Dafermos, Polygonal approximations of solutions of the initial value problem for a conservation law, *J. Math. Anal. Appl.*, **38**, (1972), 33–41.

[12] R. J. DiPerna, Global existence of solutions to nonlinear hyperbolic systems of conservation laws, *J. Differential Equations*, **20**: 1, (1976), 187–212.

[13] H. Holden and N. H. Risebro, *Front tracking for Hyperbolic Conservation Laws*, New York: Springer, 2002.

[14] H. K. Jessen, On exact solutions of rarefaction-rarefaction interactions in compressible isentropic flow, *J. Math. Fluid Mech.*, **19**: 4 (2017), 685-708.

[15] P. Lax, Development of singularities of solutions of nonlinear hyperbolic partial differential equations, *J. Mathematical Phys.*, **5**:5 (1964) 611-613.

[16] L. Lin, Vacuum states and equidistribution of the random sequence for Glimm's scheme, *J. Math. Anal. Appl.*, **124**:1, (1987), 117-126.

[17] L. Lin, On the vacuum state for the equations of isentropic gas dynamics, *Math. Anal. Appl.*, **121**:2 (1987), 406-425.

[18] T. P. Liu and J. Smoller, On the vacuum state for the isentropic gas dynamics equations, in *Appl. Math.*, **1**:4 (1980), 345-359.

[19] T. P. Liu, Z. Xin and T. Yang, Vacuum states for compressible flow, *Discrete Contin. Dynam. Systems*, **4** :1, (1998), 1–32,

[20] B. Riemann, *Ueber die Fortpflanzung ebener Luftwellen von endlicher Schwingungsweite*, Abhandlungen der Kniglichen Gesellschaft der Wissenschaften zu Gttingen, **8** (1860), 43.

[21] B. Temple and R. Young, A paradigm for time-periodic sound wave propagation in the compressible Euler equations, *Methods Appl. Anal.*, **16**:3 (2009) 341-364.

[22] C. Tsikkou, Sharper total variation bounds for the $p$-system of fluid dynamics, *J. Hyperbolic Differ. Equ.*, **8**: 2, (2011),173–232.

[23] D. Wagner, Equivalence of the Euler and Lagrangian equations of gas dynamics for weak solutions, *J. Differential Equations*, **68**: 1, (1987), 118–136.



*E-mail address*: gengchen@ku.edu

*E-mail address*: panrh@math.gatech.edu

*E-mail address*: zhus@maths.ox.ac.uk